YMTHE, Volume *26*

Supplemental Information

miR-210 Enhances the Therapeutic Potential of Bone-Marrow-Derived Circulating Proangiogenic Cells in the Setting of Limb Ischemia

Marie Besnier, Stefano Gasparino, Rosa Vono, Elena Sangalli, Amanda Facoetti, Valentina Bollati, Laura Cantone, Germana Zaccagnini, Biagina Maimone, Paola Fuschi, Daniel Da Silva, Michele Schiavulli, Sezin Aday, Massimo Caputo, Paolo Madeddu, Costanza Emanueli, Fabio Martelli, and Gaia Spinetti

Supplemental Figures

Besnier, Gasparino, Vono et al. Title: MicroRNA-210 enhances the therapeutic potential of bone marrow-derived circulating proangiogenic cells in the setting of limb ischemia.

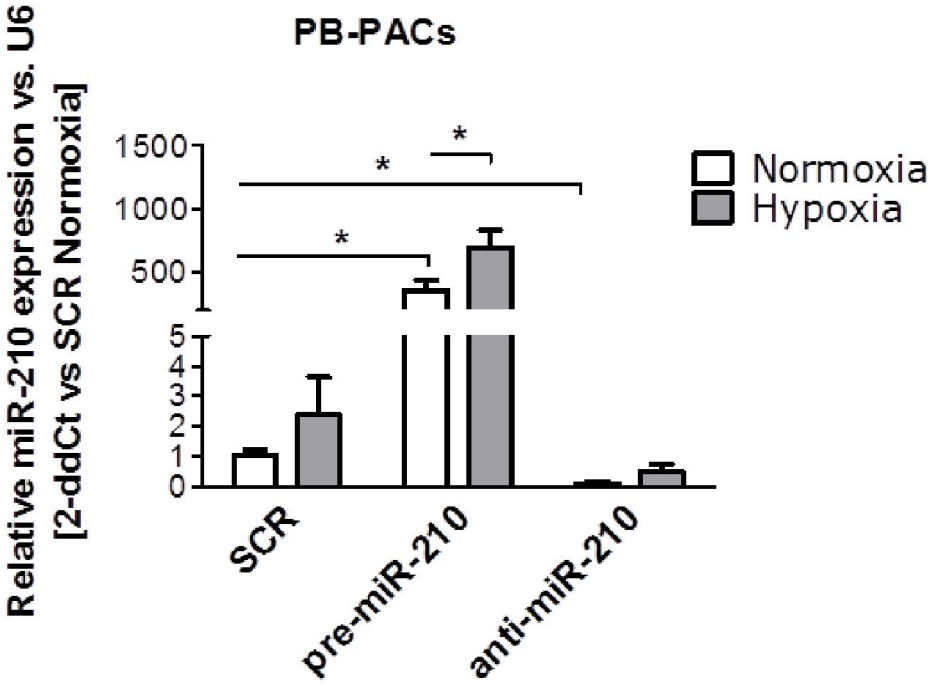

Supplementary figure I. Efficiency of miR-210 modulation in human PB-PACs. PB-PACs were transfected with pre-miR-210, anti-mir-210 or a scramble control sequence. Bar graph of relative miR-210 expression in control (scramble, SCR), pre-miR-210 and anti-miR-210 transfected PB-PACs. *p<0.05. Data shown as mean±SEM, N=4 donors. U6 snRNA used as a normalyzer

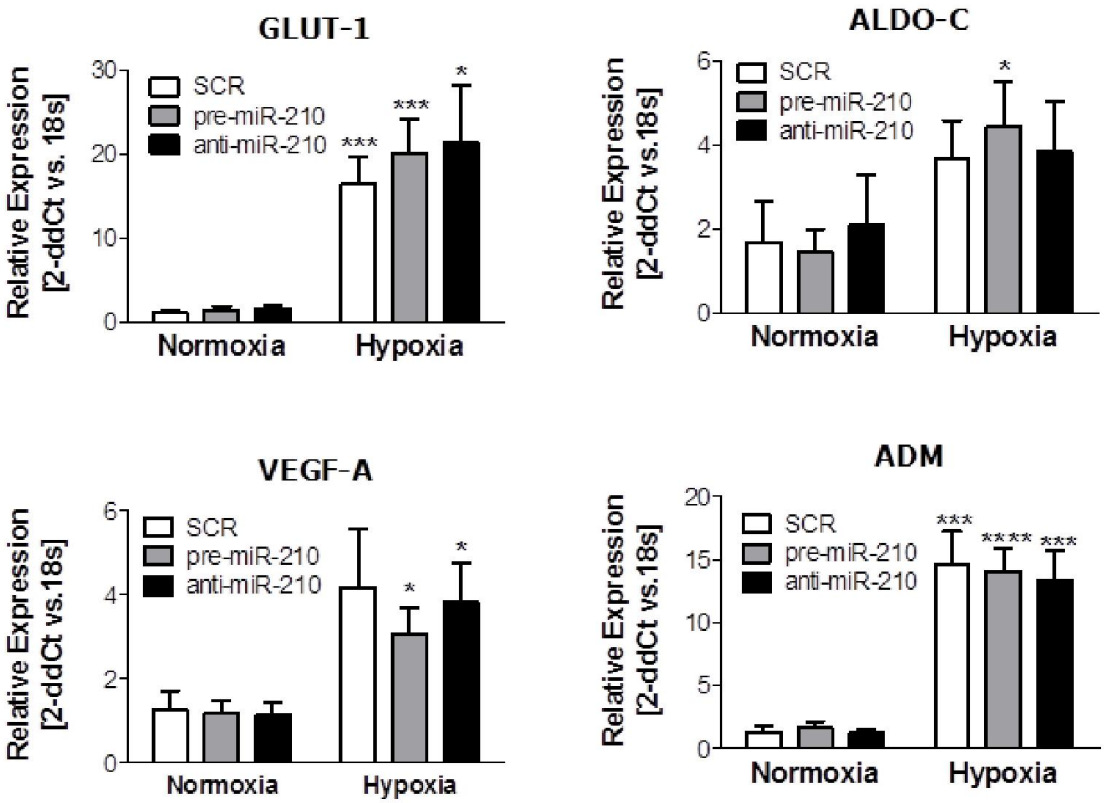

Supplementary figure II. miR-210 modulation is not associated with changes in the HIF-1a targets in adult PACs. Cells were transfected with pre-miR-210, anti-mir-210 or a scramble. After 48h, mRNA expression of *GLUT-1, ALDO-C, VEGF-A* and *ADM* was assessed by qRT-PCR over 18s housekeeping gene. Bar graph of average relative abundance of HIF1a-associated genes measured by real time q-PCR. *p<0.05; ***p<0.001; ****p<0.0001 vs. Normoxia. Data shown as mean±SEM, N=6 donors.

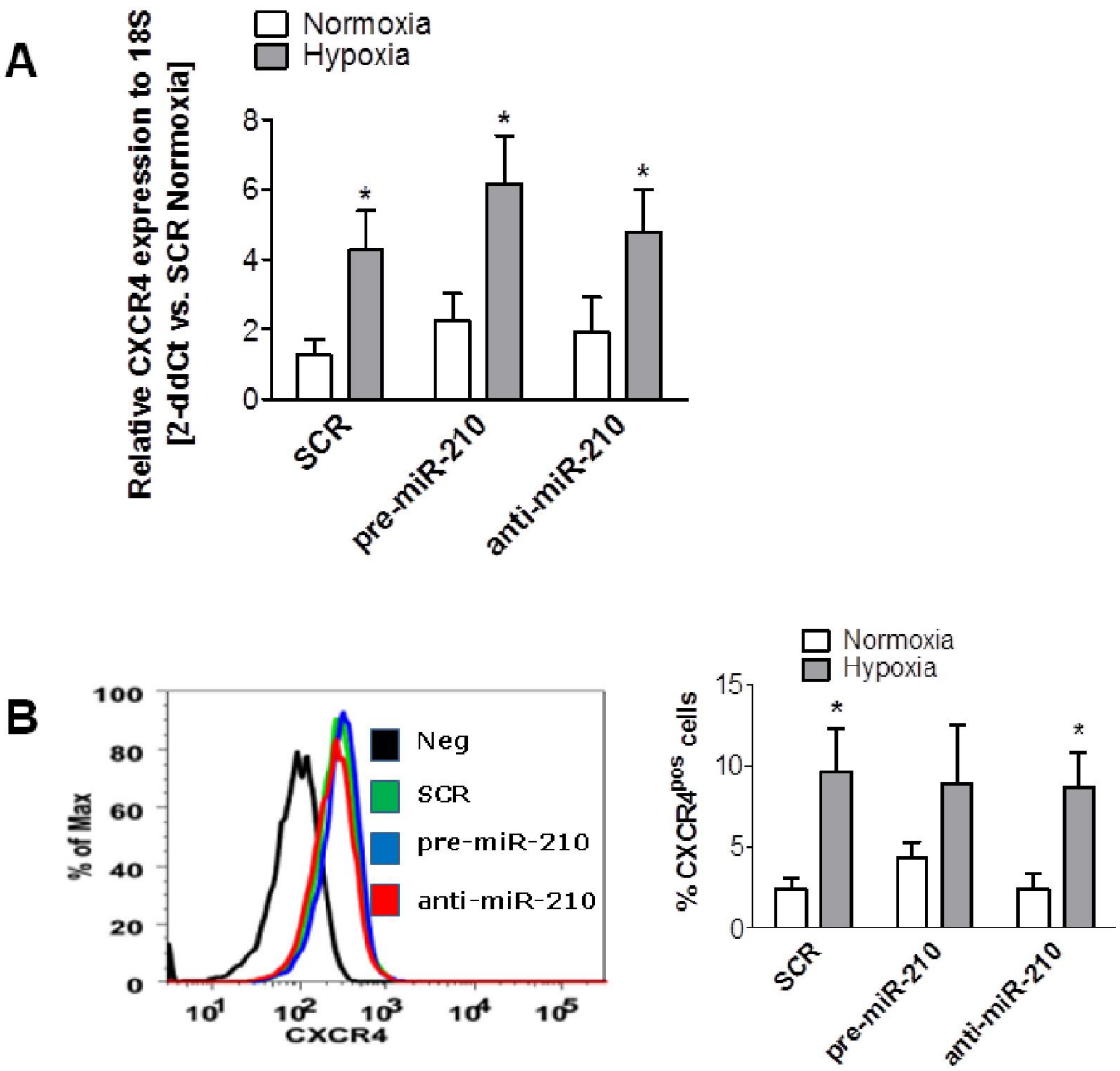

Supplementary figure III. The expression of the SDF-1a receptor CXCR4 is not altered by miR-210 expressional changes in PB-PACs cultured under hypoxia or normoxia. A) Bar graph showing CXCR4 mRNA expression in PACs engineered with pre- or anti-miR-210 and scramble (SCR). **B**) Representative flow cytometric analysis (left) and graph of average percentage of CXCR4-positive PB-PACs (right). Data shown as mean±SEM, N=6 donors. *p<0.05 vs. normoxia in both panels.

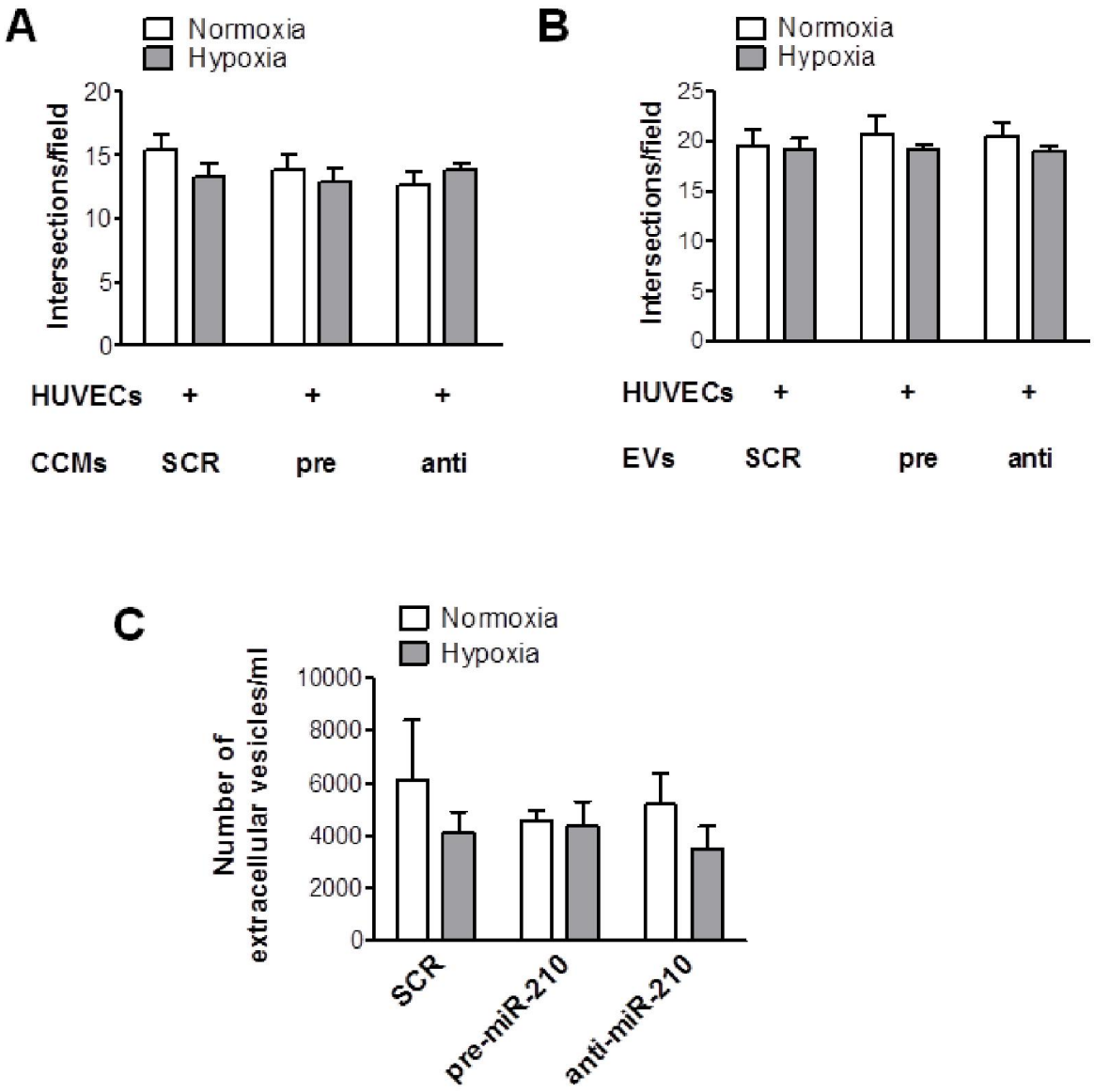

Supplementary figure IV. **Characterization of the PB-PACs paracrine activity in the Matrigel assay.** Bar graph shows the number of HUVEC intersections on Matrigel, when exposed to the **A**) unfractioned conditioned cell medium (CCM) or **B**) the CCM-derived extracellular vesicles (EVs) of engineered PACs kept under normoxia or hypoxia. **C**) The abundance of secreted EVs does not change with miR-210 expressional changes. Bar graph of average EV abundance measured by NanoSight in PAC CCMs . Data shown as mean±SEM, N=4 donors for all experiments.

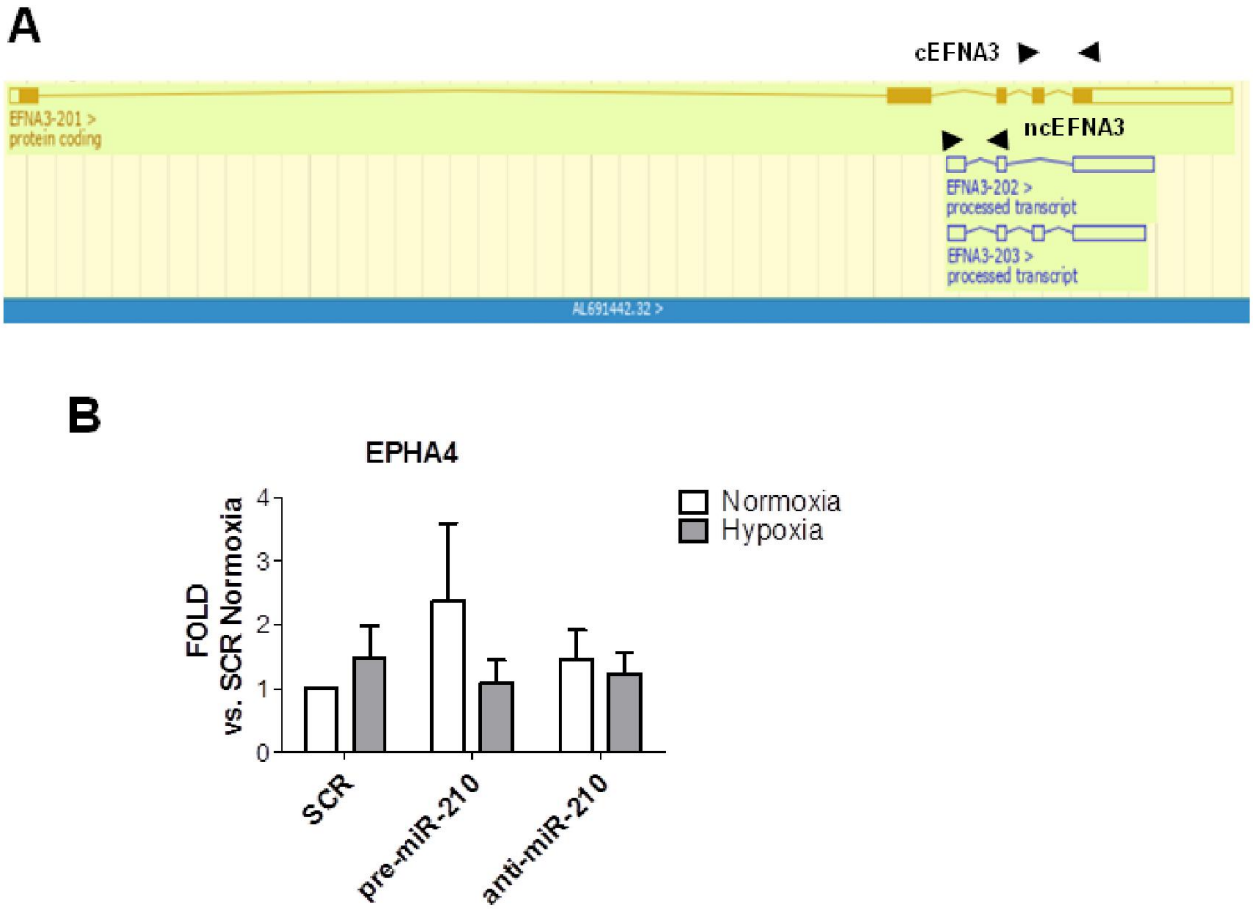

Supplementary figure V. Analysis of hypoxia and miR-210 modulation on coding and non-coding EFNA3 isoforma. Coding (cEFNA3) and non-coding (ncEFNA3) EFNA3 isoforms were analyzed by qPCR in PB-PACs. **A**) The figure shows the position of cEFNA3 and ncEFNA3A primers on the EFNA3 gene (Ensembl sequence). **B**) Analysis of EFNA3 receptor EPHA4 expression in PB-PACs under normoxia and hypoxia following miR-210 modulation. Data expressed as mean±SEM of qPCR analysis vs. UCB as housekeeping gene, N=4 donors.

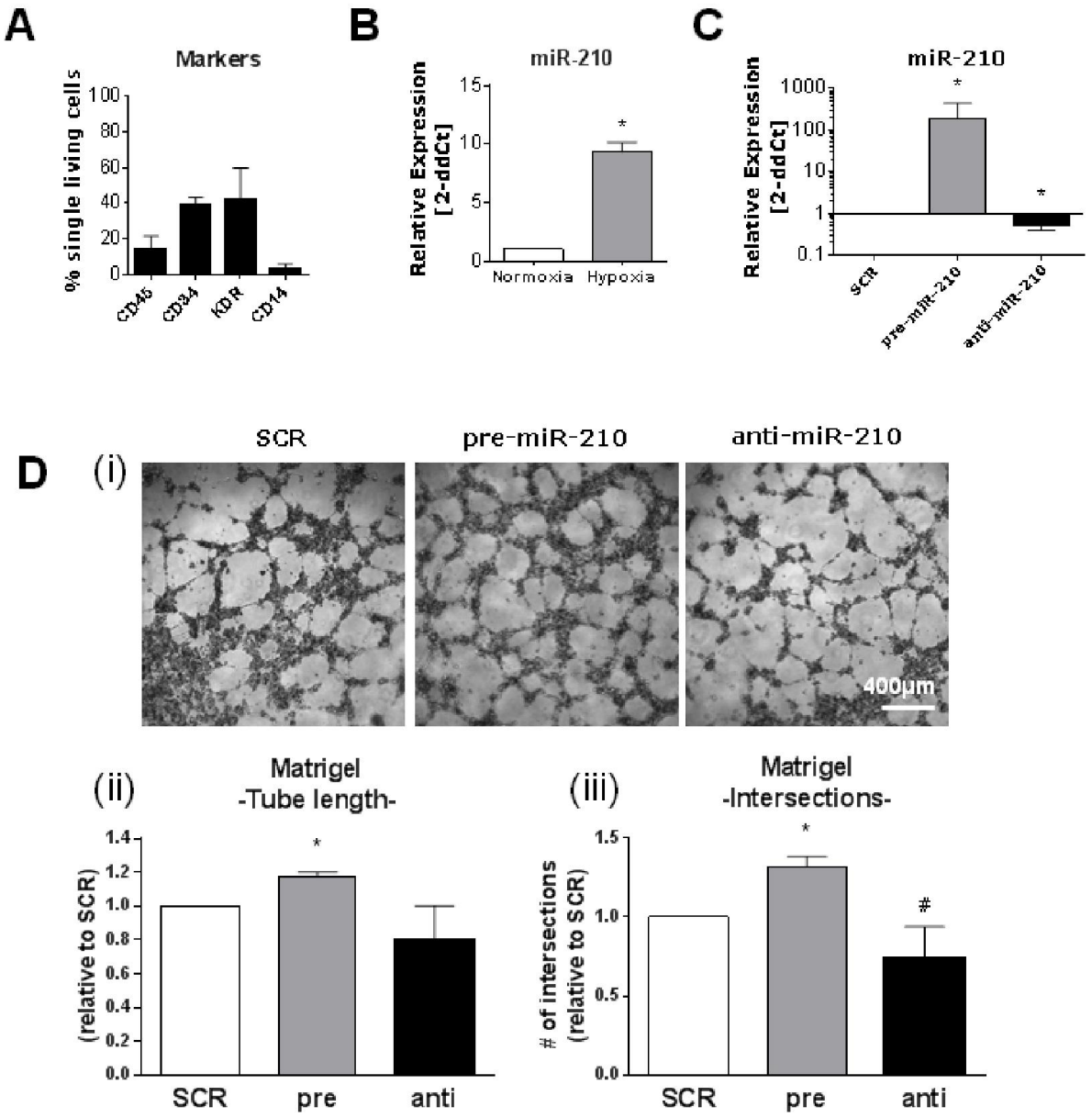

Supplementary figure VI. Characterisation of umbilical cord (UBC)-PACs and effect of modulation of miR-210 expression on PACs activity. A) Flow cytometric measurement of progenitor markers, expressed in %, of single and living cells (data shown as mean±SEM, N=3). **B**) Relative expresson of miR-210 under normoxia and hypoxia or **C**) after transfection with scramble (SCR), pre-miR-210 (pre) and anti-miR-210 (anti) in UBC-PACs. Bar graph of relative expression to snU6 shown as mean±SEM, (N=3). **D**) miR-210 facilitates HUVECs networking: (**i**) Representative pictures, scale bar: 400µm. Bar graph of average endothelial tube length (**ii**) and intersection (**iii**) ±SEM of HUVECs cultured in the presence of UBC-PAC. Data are represented as relative to each SCR control donor (N=3). *p<0.05 *vs.* SCR control or normoxia control. $^{\#}$p<0.05 *vs.* pre-miR-210 condition.

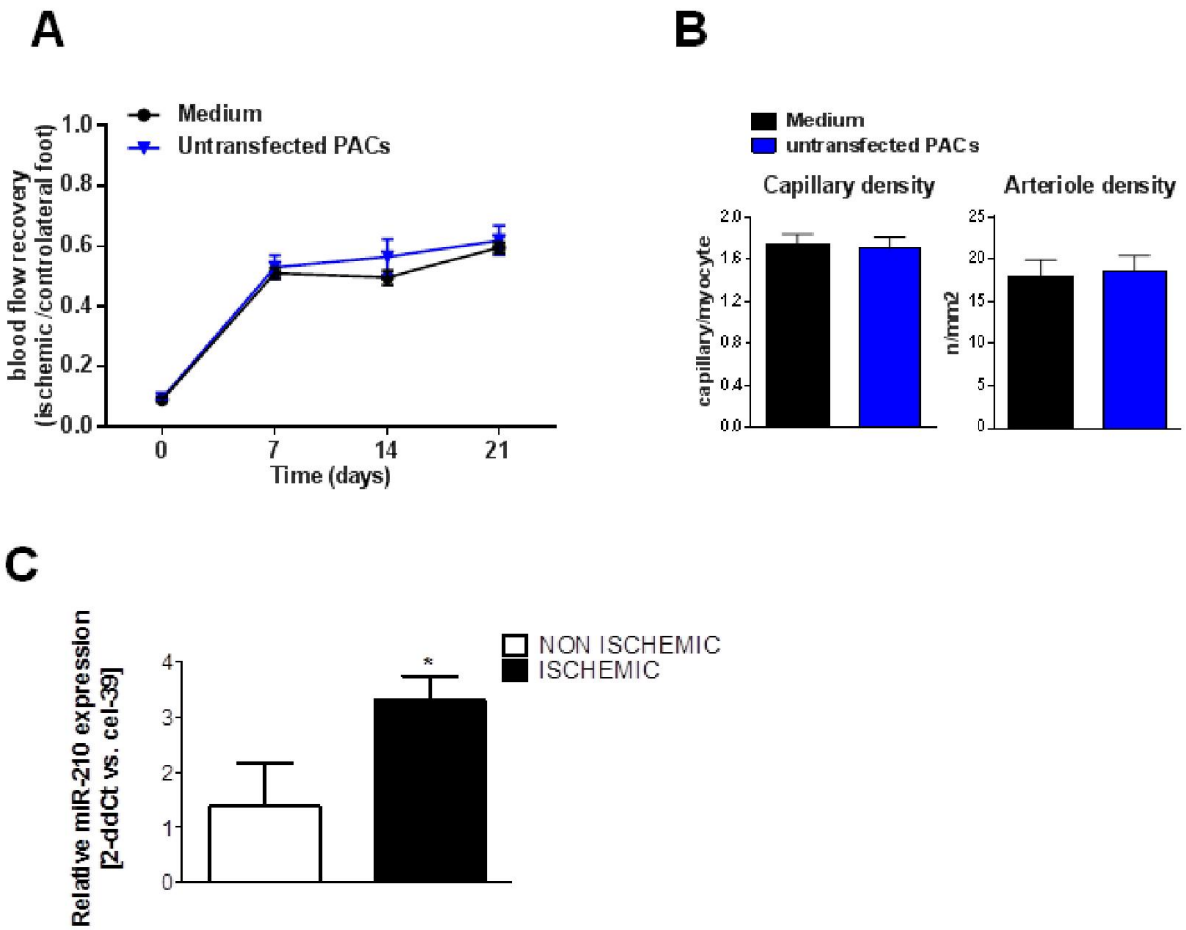

Supplementary figure VII. Untransfected PACs therapy does not increase vascular repair in our immunocompromised mouse model of unilateral limb ischemia. Untransfected PACs or fresh cell medium were injected in the ischemic adductor muscle of mice with surgically induced unilateral limb ischemia. **A**) Posti-schemic blood flow recovery: Time course of blood flow recovery (calculated as the ratio of blood flow in ischemic to contralateral foot) measured by color laser Doppler (n=11-12/group). **B**) Analyses of capillary and arteriole density in ischemic muscles at 21 days post-ischemia (n=6/group). **C**) Bar graph of average relative expression of mature miR-210 normalized by cel-miR-39 spike-in, in the plasma of CD57Bl6 mice non ischemic (N=3) and 3 days after hindlimb ischemia (ischemic, N=5). * $p<0.05$. Data are expressed as mean±SEM.